



*Citation for published version:*

Prasse, C, Wenk, J, Jasper, JT, Ternes, TA & Sedlak, DL 2015, 'Co-occurrence of photochemical and microbiological transformation processes in open-water unit process wetlands', *Environmental Science & Technology*, vol. 49, no. 24, pp. 14136-14145. <https://doi.org/10.1021/acs.est.5b03783>

*DOI:*

[10.1021/acs.est.5b03783](https://doi.org/10.1021/acs.est.5b03783)

*Publication date:*

2015

*Document Version*

Early version, also known as pre-print

[Link to publication](#)

This document is the unedited Author's version of a Submitted Work that was subsequently accepted for publication in *Environmental Science and Technology*, copyright © American Chemical Society after peer review. To access the final edited and published work see <http://pubs.acs.org/doi/10.1021/acs.est.5b03783>

**University of Bath**

### **Alternative formats**

If you require this document in an alternative format, please contact:  
[openaccess@bath.ac.uk](mailto:openaccess@bath.ac.uk)

**General rights**

Copyright and moral rights for the publications made accessible in the public portal are retained by the authors and/or other copyright owners and it is a condition of accessing publications that users recognise and abide by the legal requirements associated with these rights.

**Take down policy**

If you believe that this document breaches copyright please contact us providing details, and we will remove access to the work immediately and investigate your claim.

# **Co-occurrence of Photochemical and Microbiological Transformation Processes in Open-Water Unit Process Wetlands**

Carsten Prasse<sup>1,2</sup>, Jannis Wenk<sup>1,3</sup>, Justin T. Jasper<sup>1</sup>,  
Thomas A. Ternes<sup>2</sup>, David L. Sedlak<sup>1,\*</sup>

<sup>1</sup> ReNUWIt Engineering Research Center and Department of Civil & Environmental Engineering,  
University of California at Berkeley, Berkeley, California 94720, United States

<sup>2</sup> Department of Aquatic Chemistry, Federal Institute of Hydrology (BfG), Koblenz, Germany

<sup>3</sup> Department of Chemical Engineering and Water Innovation & Research Centre (WIRC),  
University of Bath, Claverton Down, Bath BA2 7AY, United Kingdom

\* Corresponding author: [sedlak@berkeley.edu](mailto:sedlak@berkeley.edu)

To be submitted to Environmental Science & Technology

# Co-occurrence of Photochemical and Microbiological Transformation Processes in Open-Water Unit Process Wetlands

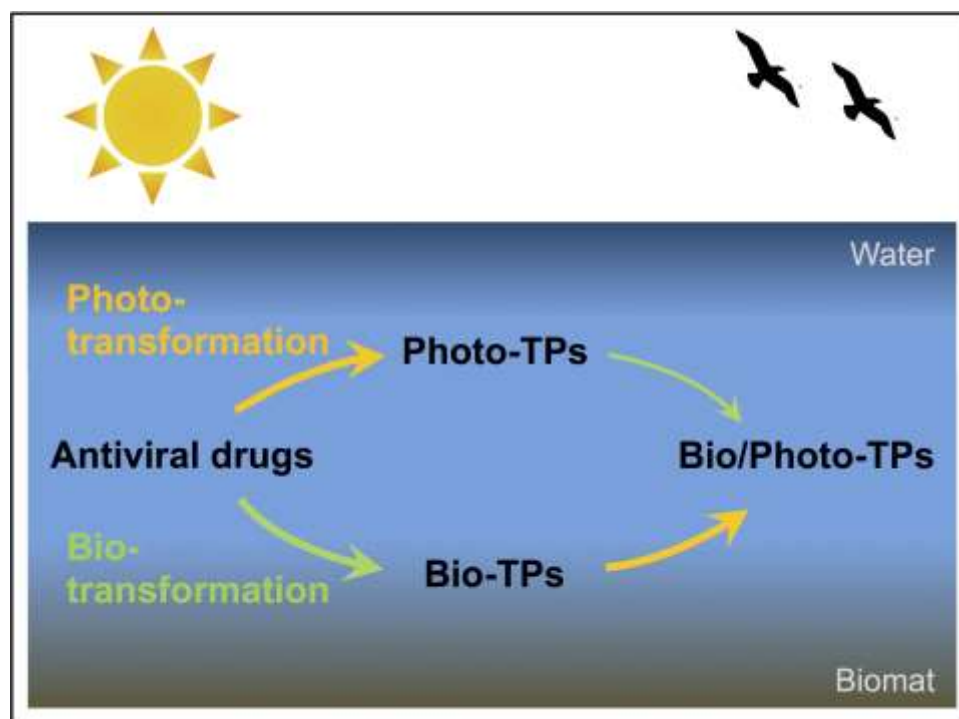
Carsten Prasse<sup>1,2</sup>, Jannis Wenk<sup>1,3</sup>, Justin T. Jasper<sup>1</sup>, Thomas A. Ternes<sup>2</sup>, David L. Sedlak<sup>1\*</sup>

<sup>1</sup> ReNUWIt Engineering Research Center and Department of Civil & Environmental Engineering, University of California at Berkeley, Berkeley, California 94720, United States

<sup>2</sup> Department of Aquatic Chemistry, Federal Institute of Hydrology (BfG), Koblenz, Germany

<sup>3</sup> Department of Chemical Engineering and Water Innovation & Research Centre (WIRC), University of Bath, Claverton Down, Bath BA2 7AY, United Kingdom

\*Corresponding author: sedlak@berkeley.edu



16  
17  
18  
19  
20

21 **Abstract**

22 The fate of anthropogenic trace organic contaminants in surface waters can be complex due  
23 to the presence of multiple parallel and consecutive transformation processes. In this  
24 study, the removal of five antiviral drugs (i.e., abacavir, acyclovir, emtricitabine, lamivudine  
25 and zidovudine) via both bio- and photo-transformation processes was investigated in  
26 laboratory microcosm experiments simulating an open-water unit process wetland  
27 receiving municipal wastewater effluent. The relative importance of the two  
28 transformation processes was strongly compound dependent. Phototransformation was  
29 the main removal mechanism for abacavir, zidovudine and emtricitabine with half-lives  
30 ( $t_{1/2,photo}$ ) in wetland water of 1.6 h, 7.6 h and 25 h, respectively. In contrast, removal of  
31 acyclovir and lamivudine was mainly attributable to slower microbial processes ( $t_{1/2,bio} =$   
32 74 h and 120 h, respectively). Identification of transformation products via high-resolution  
33 mass-spectrometry revealed that bio- and photo-transformation reactions took place at  
34 different moieties of the molecules. For abacavir and zidovudine, rapid transformation was  
35 attributable to the high reactivity of the cyclopropylamine and azido moiety, respectively.  
36 Despite substantial differences in kinetics of different antiviral drugs, biotransformation  
37 reactions mainly involved oxidation of hydroxyl groups to the corresponding carboxylic  
38 acids. Phototransformation rates of parent antiviral drugs and their biotransformation  
39 products were similar, indicating that prior exposure to microorganisms (e.g., in a  
40 wastewater treatment plant or a vegetated wetland) would not affect the rate of  
41 transformation of the part of the molecule that was susceptible to phototransformation.  
42 However, phototransformation strongly affected the rates of biotransformation of the  
43 hydroxyl groups, which in some cases resulted in greater persistence of abacavir and  
44 acyclovir phototransformation products.

45  
46  
47  
48  
49  
50  
51

## 52 **Introduction**

53 The discharge of municipal wastewater effluents into surface waters can result in the  
54 presence of trace organic contaminants at concentrations that pose potential risks to  
55 aquatic ecosystems and drinking water resources. After their release, many trace organic  
56 contaminants are attenuated by biological and photochemical processes. Although these  
57 processes often occur simultaneously or sequentially in the environment, most studies  
58 have considered the occurrence of only one transformation process at a time.<sup>1-4</sup> Thus, it is  
59 difficult to predict which transformation products are formed and whether or not  
60 transformation reactions occurring at one moiety alter the kinetics of subsequent  
61 transformation reactions. Furthermore, if partial transformation of a compound enhances  
62 the reactivity of other moieties, interaction of transformation processes could result in  
63 changes in the distribution of transformation products as well as their rates of removal. For  
64 example, carbamazepine, a compound that is particularly resistant to biotransformation is  
65 slowly transformed upon exposure to sunlight via direct photolysis and reaction with  
66  $\cdot\text{OH}$ .<sup>5,6</sup> This leads to the formation hydroxylated derivatives<sup>7</sup> which are more easily  
67 biodegraded than the parent compound.<sup>8</sup>

68 Open water unit process wetlands have been developed as a polishing treatment step for  
69 municipal wastewater effluents.<sup>9</sup> These managed natural systems utilize sunlight to  
70 remove trace organic compounds and deactivate pathogens.<sup>10-12</sup> In addition,  
71 microorganisms in the biomat formed at the bottom of these treatment basins reduce  
72 nitrate and contribute to aerobic biodegradation of trace organic contaminants.<sup>13,14</sup> To  
73 assess the importance of the co-occurrence of biological and photochemical transformation  
74 reactions to reaction kinetics and product distribution, the fate of five antiviral drugs (i.e.,  
75 abacavir, emtricitabine, lamivudine, zidovudine and acyclovir, see Figure 1) was studied  
76 under conditions comparable to those encountered in open-water unit process wetlands.

77 Antiviral drugs were chosen because they are widely used for the treatment of diseases  
78 such as herpes, hepatitis and HIV, and have been detected at concentrations above  $1 \mu\text{g L}^{-1}$   
79 in municipal wastewater effluents.<sup>15-18</sup> No information about potential environmental  
80 effects resulting from the release of these compound into the aquatic environment is  
81 available so far. Furthermore, little is known about the effects of these compounds on

82 environmental viruses, a group of microorganisms that play a very important role in  
83 aquatic ecosystems.<sup>19</sup>

84 By investigating transformation kinetics and transformation mechanisms under conditions  
85 comparable to those encountered in open-water unit process wetlands it is possible to gain  
86 insight into how simultaneously occurring bio- and photo-transformation reactions affect  
87 the overall fate of antiviral drugs in sunlit surface waters. These compounds also serve as  
88 models for other families of compounds that contain moieties that are susceptible to bio-  
89 and phototransformation.

90

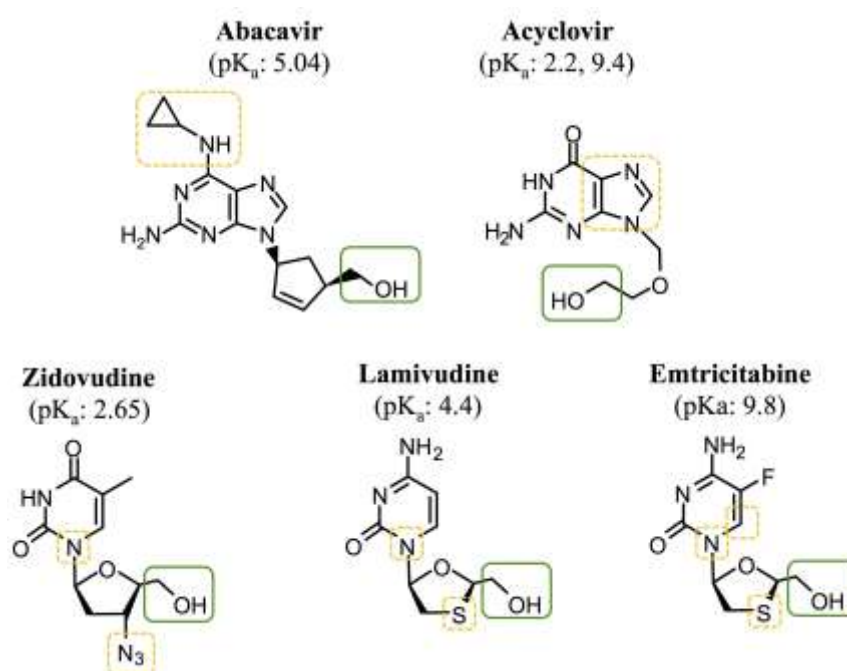


Figure 1. Antiviral drugs and their most likely sites of proposed photo- (□) and biotransformation (□) reactions.

91

## 92 **Materials and Methods**

### 93 *Chemicals*

94 Analytical reference standards of antiviral drugs and stable isotope-labeled analogues used  
95 as internal standards (purity > 99%) were purchased from Toronto Research Chemicals  
96 (Ontario, Canada). All other chemicals and solvents were obtained from Fisher Scientific  
97 (Fairlawn, NJ).

98

99 *Wetland water sampling conditions*

100 Phototransformation experiments were conducted in water collected from a pilot-scale  
101 open-water unit process wetland located in Discovery Bay, CA. The facility treats about  
102 10,000 gallons per day ( $4.4 \times 10^{-4} \text{ m}^3 \text{ s}^{-1}$ ) of nitrified wastewater effluent from an adjacent  
103 municipal wastewater treatment plant. Details about the open-water unit process wetland  
104 were described previously.<sup>10,13</sup> Water collected from the open-water wetland typically  
105 contained 10 - 20 mg L<sup>-1</sup> -N NO<sub>3</sub><sup>-</sup>, 5 - 10 mg L<sup>-1</sup>-C DOC, and 60 - 80 mg L<sup>-1</sup>-C dissolved  
106 inorganic carbon (HCO<sub>3</sub><sup>-</sup> and CO<sub>3</sub><sup>2-</sup>). Samples for laboratory irradiation experiments were  
107 collected from the mid-point of the wetland. All samples were filtered through pre-rinsed  
108 1µm (nominal pore size) glass fiber filters (Whatman) and were stored in the dark at 4°C  
109 until analysis, which occurred within 5 days.

110

111 *Laboratory photo- and biotransformation experiments (or: Determination of photo- and*  
112 *biotransformation kinetics)*

113 Irradiation experiments were performed using a collimated beam Oriel Solar Simulator  
114 (Spectra Physics, serial no. 91194) equipped with a 1000 W Xe lamp and either two  
115 successive atmospheric attenuation filters (Spectra Physics, serial no. 81088 & 81017) or  
116 one atmospheric and one UVB-filter (Spectra Physics, serial no. 81088 & 81050). Spectral  
117 irradiance was routinely measured with a spectroradiometer (RPS 380, International light)  
118 at different locations of the irradiated area to assess variability, which was always < 5%.  
119 Details on lamp irradiance energies and the spectra of different configurations are given in  
120 section 1.1 of the Supporting Information (SI). Irradiation experiments were carried out in  
121 100mL black-painted glass beakers that were placed in a water bath at constant  
122 temperature ( $18 \pm 2^\circ\text{C}$ ). Initial concentrations of antivirals of approximately 0.5 µM were  
123 used for all kinetics experiments. Pseudo-first order phototransformation rate constants of  
124 antivirals and photochemical probe compounds used for the quantification of reactive  
125 intermediates were calculated from the slopes of linear regression of the natural log of  
126 concentration versus time. Control experiments in the dark revealed no degradation of  
127 antiviral drugs indicating that their transformation in wetland water can solely be  
128 attributed to photochemical processes.

129 For the elucidation of biotransformation kinetics experiments beakers were additionally  
130 supplemented with 10 mL of the biomat taken from the bottom of the pilot-scale wetland  
131 and kept in the dark (see Jasper et al, for further details).

132  
133 *Direct and indirect phototransformation.* Experiments to assess direct phototransformation  
134 of antiviral drugs were conducted in buffered ultrapure water at pH-values ranging from 6  
135 to 10 (pH 6 - 8: 5 mM phosphate buffer; pH 9 - 10: 5 mM borate buffer). Samples (1 mL)  
136 were collected at regular time intervals and stored at 4°C in the dark until analysis.  
137 Electronic absorption spectra of antiviral drugs at different pH values (see Fig. S2) were  
138 recorded with a UV-2600 UV-Vis Spectrophotometer (Shimadzu) using quartz-glass  
139 cuvettes (Hellma, Germany). Further details on determination of quantum yields using the  
140 *p*-nitroanisole (PNA)/pyridine(PYR) method<sup>20</sup> and related calculations are provided in  
141 section 1.6 of the SI.

142 Indirect phototransformation of antiviral drugs was investigated by the addition of specific  
143 quenchers to wetland water: *N,N*-dimethylaniline (DMA; 10 μM) was used to scavenge CO<sub>3</sub>-  
144 radicals<sup>10</sup>, sorbic acid (2.5 mM) to scavenge excited triplet states of the dissolved organic  
145 matter (<sup>3</sup>DOM\*)<sup>21</sup>, histidine (20 mM) to scavenge singlet oxygen (<sup>1</sup>O<sub>2</sub>)<sup>22</sup> and isopropyl  
146 alcohol (IPA; 26 mM) to scavenge <sup>•</sup>OH-radicals.<sup>23</sup> In addition, experiments with specific  
147 photosensitizers and were conducted in ultrapure buffered water to determine reaction  
148 rate constants of antiviral drugs with individual reactive intermediates: For CO<sub>3</sub><sup>•-</sup> either  
149 NaNO<sub>3</sub>/NaHCO<sub>3</sub> or NaNO<sub>3</sub>/duroquinone photosensitizer methods were used.<sup>24,25</sup> The  
150 excited triplet state photosensitizers 3-methoxyacetophenone (3MAP) and anthraquinone-  
151 2-sulfonate (AQ2S) served as a proxy for <sup>3</sup>DOM\*.<sup>26</sup> Hydroxyl-radicals were generated by  
152 the irradiation of NaNO<sub>3</sub> solutions.<sup>27</sup> For <sup>1</sup>O<sub>2</sub> production Rose Bengal was used as a  
153 photosensitizer.<sup>28</sup> To further verify the role of <sup>1</sup>O<sub>2</sub>, some experiments were performed in  
154 D<sub>2</sub>O. Reaction rate constants were either determined by competition kinetics or by  
155 comparing reaction rates of antiviral drugs with those of established photochemical probe  
156 compounds (experimental details and calculations are provided in section 1.5 and 1.7). For  
157 all indirect phototransformation experiments, the concentration changes of photochemical  
158 probe compounds and antiviral drugs during irradiations were followed by HPLC-UV.  
159 Experimental and analytical details, including comprehensive results are provided in SI.



160 Given the structural similarities of antivirals with DNA bases, additional irradiation  
161 experiments were performed with adenine, 2-amino adenosine, cytosine, cytidine, guanine,  
162 thymidine and thymine (SI section 2.1.1) to obtain further information about the  
163 photoreactive moieties in the molecules and thus aid the identification of transformation  
164 products.

165  
166 *Identification of photo- and biotransformation products.* High resolution mass spectrometry  
167 (HR-MS; LTQ Orbitrap Velos, Thermo Scientific, Bremen, Germany) was used to conduct  
168 accurate MS and MS/MS analysis of transformation products of antiviral drugs. To this end,  
169 experiments at elevated concentrations (40  $\mu\text{M}$ ) were used. The LTQ Orbitrap Velos was  
170 coupled to a Thermo Scientific Accela liquid chromatography system (Accela pump and  
171 autosampler). HR-MS was conducted in the positive electrospray ionization (ESI) mode. To  
172 obtain structural information on the chemical structure of formed TPs, MS<sup>n</sup> fragmentation  
173 experiments were conducted using data dependent acquisition. Further information on the  
174 applied setup and data dependent acquisition parameters can be found in the SI (section  
175 1.2). Product formation of antiviral drugs in laboratory experiments was determined liquid  
176 chromatography tandem mass spectrometry (LC/MS/MS). Details on the analytical  
177 methods are provided in the SI (section 1.3).

178  
179 *Combined bio- and photodegradation experiments.* The fate of antiviral drugs in the  
180 presence of sunlight and microorganisms was investigated over a 72 h period in the  
181 laboratory. Amber glass beakers (250mL) were filled with 180 mL of wetland water and 20  
182 mL of freshly collected biomat material from the bottom of the Discovery Bay open-water  
183 unit process wetland. The experimental setup was the same as described above for  
184 photochemical experiments, but with three day/night cycles to simulate field conditions (8  
185 h of daily irradiation followed by 16 h in the darkness; 72 h total). Antiviral drugs were  
186 added individually at concentrations of 0.5  $\mu\text{M}$  to ensure detection of both parent antiviral  
187 compounds and their transformation products. Samples were collected at regular time  
188 intervals and stored at 4°C in the dark prior to LC/MS/MS analysis, which occurred within  
189 24 h. Further details about the analytical method can be found in the SI.

190

191 **Results and Discussion**

192 *Phototransformation in wetland water*

193 Phototransformation of the five investigated antiviral drugs in wetland water followed  
194 first-order kinetics ( $r^2 \geq 0.98$ ; Figure S4-S8). In native wetland water (pH 8.9), the fastest  
195 phototransformation was observed for abacavir ( $k_{\text{obs}} = 0.52 \pm 0.06 \text{ h}^{-1}$ ), zidovudine ( $k_{\text{obs}} =$   
196  $0.09 \pm 0.002 \text{ h}^{-1}$ ) and emtricitabine ( $k_{\text{obs}} = 0.03 \pm 0.002 \text{ h}^{-1}$ ) whereas the transformation of  
197 acyclovir and lamivudine were significantly slower ( $k_{\text{obs}} = 0.012 \pm 0.001 \text{ h}^{-1}$  and  $0.011 \pm$   
198  $0.001 \text{ h}^{-1}$ , respectively) (Figure 2). No degradation of antiviral drugs in wetland water in  
199 the dark was observed indicating that their removal was solely attributable to  
200 photochemical processes. Photosynthetic activity leads to significant diurnal fluctuations of  
201 pH in open-surface wetlands.<sup>10</sup> Therefore, phototransformation kinetics of antiviral drugs  
202 in wetland water were also determined at pH 6.5 and pH 10 (Figure 2).

203

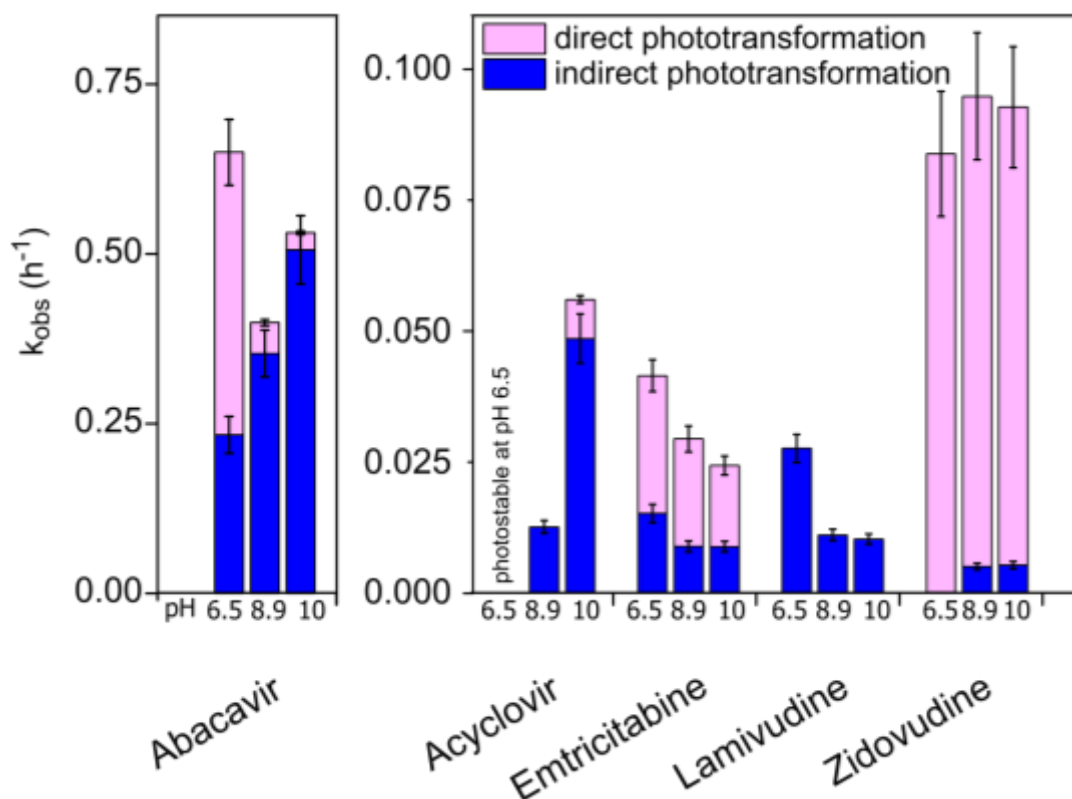


Figure 2. Phototransformation kinetics of antiviral drugs in experiments with wetland water at different pH values and contribution of direct and indirect photolysis processes by comparison with results obtained in ultrapure water. Data for wetland water are corrected for light-absorption. Error bars show 95% confidence intervals.

204

205 Phototransformation of abacavir in wetland water increased when the pH value was  
206 adjusted to 6.5 or 10. This can be attributed to higher contribution of direct photolysis due  
207 to higher quantum yields at lower pH values (i.e.  $\Phi_{app}$  is 4.2 – 11.4 times higher between pH  
208 6 – 8, compared to pH 9 and 10, SI Table S5) and faster indirect photolysis at higher pH  
209 values. Comparison of transformation kinetics with results obtained in ultrapure water  
210 revealed the dominance of indirect photodegradation processes at pH 8.9 and 10, whereas  
211 direct photolysis was more important at pH 6.5. The addition of sorbic acid and histidine  
212 significantly reduced phototransformation rates of abacavir in wetland water (Fig. S4),  
213 suggesting the involvement of  $^3\text{DOM}^*$  and  $^1\text{O}_2$  in the photochemical fate of this compound.  
214 This was also supported by experiments with specific singlet oxygen and excited triplet  
215 state sensitizers (see below). Negligible removal of the structural analogues adenine and 2-  
216 amino-adenosine further revealed that the photolability of abacavir can be attributed to the  
217 cyclopropyl-moiety (see SI section 2.1.1).

218 Rates of phototransformation of zidovudine were not affected by changes in pH.  
219 Comparison with reaction rates in both ultrapure water and wetland water in the presence  
220 of scavengers revealed the dominance of direct photolysis (Fig. S5). Similar to abacavir,  
221 comparison with the depletion of structural analogues thymine and thymidine indicated  
222 that the azide moiety was responsible for the observed photoreactivity of zidovudine as  
223 both analogues showed no removal when exposed to light (see SI section 2.1.1).

224 Phototransformation of acyclovir in wetland water increased with increasing pH.  
225 Comparison with results from ultrapure water revealed that removal at pH 8.9 was solely  
226 due to indirect photolysis, whereas at pH 10 direct photolysis was also relevant.  
227 Significantly reduced rates of acyclovir phototransformation in the presence of sorbic acid  
228 and histidine indicated the importance of  $^1\text{O}_2$  and  $^3\text{DOM}^*$  to indirect photolysis (Fig. S6). In  
229 contrast to abacavir and zidovudine, phototransformation kinetics were similar to those  
230 observed for the structural analogue guanine (SI Fig. S15). Thus, phototransformation of  
231 acyclovir can be attributed primarily to the guanine moiety.

232 For lamivudine and emtricitabine, phototransformation kinetics in wetland water  
233 decreased with increasing pH. No removal of lamivudine was observed in ultrapure water  
234 indicating that its removal was entirely attributable to indirect photolysis. Higher

235 phototransformation rates of emtricitabine relative to lamivudine further indicated the  
236 strong influence of the fluorine atom for emtricitabine's photolability. The presence of the  
237 fluorine substituent leads to a higher absorption at 300-320 nm and thus alters the  
238 compound's UV absorbance at wavelengths between 300-320 nm (SI Fig. S2). Even though  
239 the absorption spectrum of emtricitabine did not change with pH, the quantum yield  
240 steadily decreases with increasing pH (Table S5). Phototransformation of lamivudine in  
241 wetland water was fully inhibited by sorbic acid, histidine and IPA but was unaltered in the  
242 presence of DMA (Fig. S7). This indicates the importance of  $^3\text{DOM}^*$ ,  $^1\text{O}_2$  and OH-radicals for  
243 its indirect phototransformation. For emtricitabine, phototransformation rates in wetland  
244 were only affected by IPA and sorbic acid (Fig. S8), indicating that reactions with  $^1\text{O}_2$  are  
245 less important for this compound. The high photostability of its associated DNA base  
246 cytosine and nucleotide cytidine revealed the importance of structural modifications (thiol  
247 group (both compounds) and fluorine (emtricitabine)) to the observed photodegradability.

248  
249 Additional experiments with individual reactive species revealed second order reaction  
250 rates with  $\cdot\text{OH}$  at or above (abacavir, zidovudine) diffusion controlled levels ranging from  
251  $5 \cdot 10^9 - 1.1 \cdot 10^{11} \text{ M}^{-1}\text{s}^{-1}$  (Table 1). Antiviral compounds were reactive with  $\text{CO}_3^{\cdot-}$ , at rates  
252 between  $1.2 \cdot 10^6 - 1.2 \cdot 10^9 \text{ M}^{-1}\text{s}^{-1}$ , while only abacavir ( $1.2 \cdot 10^9 \text{ M}^{-1}\text{s}^{-1}$ ) and acyclovir ( $1.2 \cdot 10^7$   
253  $\text{M}^{-1}\text{s}^{-1}$ ) were obviously reactive with  $^1\text{O}_2$ . With the exception of abacavir, no depletion of  
254 antiviral compounds was observe in the presence of the model triplet photosensitizer  
255 3MAP but in presence of AQ2S at rates similar or higher than the reference probe  
256 compound TMP, indicating a selective reactivity with excited triplet states. In order to  
257 check the plausibility of results for indirect phototransformation and obtain further  
258 indications for the role of different reactive species, steady-state concentrations of reactive  
259 species measured in wetland water (Table S4) were multiplied with measured second-  
260 order reaction rate constants of antivirals with  $^1\text{O}_2$ ,  $\cdot\text{OH}$  and  $\cdot\text{CO}_3^-$ , respectively (Table 1).  
261 Based on this estimation revealed for abacavir that at pH 8.9 approximately 60% of its  
262 indirect photodegradation in wetland water can be attributed to  $^1\text{O}_2$ . For acyclovir the  
263 important role of  $^1\text{O}_2$  for photodegradation was also strengthened, although the prediction  
264 overestimates depletion rates by a factor two. For emtricitabine and lamivudine the

265 contribution of  $^1\text{O}_2$ ,  $\cdot\text{OH}$  and  $\cdot\text{CO}_3^-$  can be assumed negligible, emphasizing the role of  $^3\text{DOM}^*$   
 266 and corroborating results of quenching experiments.  
 267

Table 1. Quantum yields (pH 9) and apparent second-order reaction rate constants of indirect phototransformation of antiviral drugs via reaction with  $^1\text{O}_2$ ,  $\cdot\text{OH}$ ,  $\cdot\text{CO}_3^-$  and excited triplet states (given relative to the degradation of the  $^3\text{Sens}^*$  probe compound TMP). Quantum yields of antiviral drugs at pH 6-8 and pH 10 can be found in SI Table S5.

	[M Es <sup>-1</sup> ]	[M <sup>-1</sup> s <sup>-1</sup> ]				[-]	
	$\Phi_{\text{app}}$ (pH 9)	$^1\text{O}_2$	$\cdot\text{OH}$	$\cdot\text{CO}_3^-$ ( $\text{NO}_3^- + \text{HCO}_3^-/\text{CO}_3^{2-}$ )	$\cdot\text{CO}_3^-$ (DQ)	$^3\text{SENS}^*$ (AQ2S)	$^3\text{SENS}^*$ (MAP)
<b>Abacavir</b>	0.014 (±0.003)	$1.2 \times 10^9$ (± 18%)	$1.1 \times 10^{11}$ (± 3%)	$1.2 \times 10^9$ (± 4%)	- <sup>a</sup>	4.88	13.5
<b>Zidovudine</b>	0.45 (±0.15)	n.d.	$1.3 \times 10^{10}$ (± 2%)	$2.4 \times 10^6$ (± 5%)	$1.3 \times 10^6$ (± 4%)	0.62	n.d.
<b>Acyclovir</b>	0.01 (±0.005)	$1.2 \times 10^7$ (± 25%)	$5.0 \times 10^9$ (± 2%)	$1.2 \times 10^8$ (± 2%)	$6.3 \times 10^7$ (± 4%)	0.08	n.d.
<b>Emtricitabine</b>	0.016 (±0.005)	n.d.	$9.3 \times 10^9$ (± 2%)	$3.0 \times 10^6$ (± 4%)	$4.3 \times 10^6$ (± 12%)	2.03	n.d.
<b>Lamivudine</b>	n.d.	n.d.	$9.2 \times 10^9$ (± 1%)	$1.2 \times 10^6$ (± 3%)	$1.7 \times 10^6$ (± 3%)	1.86	n.d.

268 n.d.: not detected above level of uncertainty; <sup>a</sup> not applicable due to reaction of abacavir with DQ also in the dark

269  
 270 *Comparison of photo- vs biotransformation rates*  
 271 Dark experiments conducted with wetland water in the presence of biomat material  
 272 indicated that biotransformation rates varied considerably among antiviral drugs.  
 273 Biotransformation half-life times ( $t_{1/2,\text{bio}}$ ) ranged from 74 h for acyclovir to 500 h (21 d) for  
 274 emtricitabine (Fig. 3; Fig. S13). Under typical wetland treatment conditions (i.e., hydraulic  
 275 retention times of 2-3 days), significant biological attenuation of acyclovir and abacavir is  
 276 expected whereas for the other antiviral drugs removal via microbial processes is unlikely  
 277 to be an important removal pathway. Comparison of transformation rates of antiviral drugs  
 278 in the dark to those observed in irradiated wetland water indicated that  
 279 phototransformation processes were dominant for abacavir, zidovudine and emtricitabine,  
 280 while for acyclovir and lamivudine biotransformation was similar or more important than  
 281 photolysis during typical summertime conditions (Fig. 3).  
 282

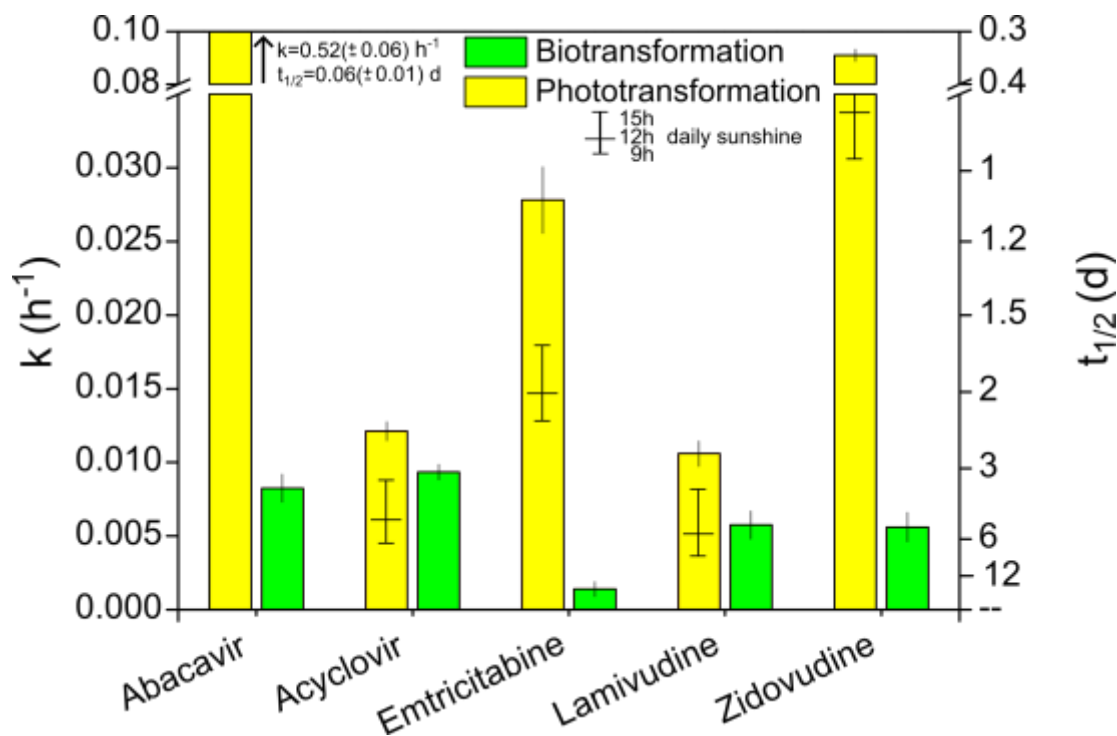


Figure 3. Photo- and biotransformation rate constants  $k$  ( $\text{h}^{-1}$ ) and associated half-life time  $t_{1/2}$  (d) of antiviral drugs in laboratory experiments. Small bars within phototransformation columns indicate half-life times based on daily sunshine hours (9-15 hours). For the determination of biodegradation half-life times experiments were conducted in the presence of biomat in the dark. Error bars represent 95% confidence intervals obtained from linear regressions.

283

#### 284 Transformation of abacavir

285 HRMS analysis indicated that four primary transformation products (TP318, TP288, TP284  
 286 and TP246) were formed during photolysis of abacavir in wetland water (SI section 2.2;  
 287 Table S7). In agreement with results obtained for the structural analogues 2-amino-  
 288 adenosine and adenine, fragmentation patterns of TP318, TP288 and TP246 revealed that  
 289 the cyclopropylamine moiety was the main site of reaction, leaving the 2-amino-adenine  
 290 (fragments:  $m/z$  151.073, 134.046 and 109.051) and the 2-cyclopenten-1-methanyl  
 291 moieties (fragments:  $m/z$  95.353 and 79.054) unaltered.

292 Exact mass calculations of TP318 showed addition of two oxygen atoms to the cyclopropyl  
 293 moiety ( $\Delta m$  +31.9898 Da). Results from  $\text{MS}^2$  experiments were consistent with the scission  
 294 of the cyclopropyl ring and the presence of a terminal hydroxyl group, as indicated by the  
 295 cleavage of  $\text{H}_2\text{O}$  and  $\text{CH}_2\text{O}$ .

296 For TP288, MS data suggested modification of the cyclopropyl moiety via loss of one carbon  
 297 atom and the addition of one oxygen atom, leading to the formation of an acetamide,

298 whereas TP246 was formed via cleavage of the cyclopropyl ring. The chemical structure of  
299 TP246 was confirmed by comparison with a commercially available reference standard.  
300 The exact mass and fragmentation pattern of TP284 was consistent with loss of two  
301 protons from either the cyclopropylamine or the 2-amino-adenosine moiety (fragments  
302 m/z 149.069 and 189.088 instead of m/z 151.073 and 191.104 compared to abacavir and  
303 the other TPs). Considering the high photolability of the cyclopropyl moiety, these  
304 structural changes were most likely due to the formation of a cyclopropylimine.

305 To assess the relative importance of direct and different indirect photolysis processes for  
306 formation of the observed abacavir transformation products, their formation was  
307 investigated in buffered water (direct photolysis only), wetland water (direct and indirect  
308 photolysis), and wetland water in the presence of different reactive intermediate  
309 scavengers. The results revealed that both direct and indirect photolysis of abacavir  
310 produced the same suite of TPs at similar relative concentrations, despite the fact that the  
311 disappearance of the parent compound was significantly accelerated in the presence of  
312 DOM and individual reactive intermediates (Fig. S17 & S18). Similar results were observed  
313 for irgarol, an algaecide that is structurally similar to abacavir, suggesting that the  
314 cyclopropylamine moiety is the main site of reaction under all conditions.<sup>29</sup>  
315 Photodegradation experiments in buffered ultrapure water with different optical filters  
316 indicated that wavelengths below 320 nm preferentially led to cleavage of the cyclopropyl  
317 moiety (TP246), whereas wavelengths above 320 nm (UV-A & visible light) led to scission  
318 of the cyclopropyl ring followed by partial oxidation (TP318) (Fig. S19).

319 These findings suggest that phototransformation of abacavir is initiated by a one electron  
320 oxidation of the cyclopropylamine moiety, leading to the formation of a  
321 cyclopropylaminium radical cation,<sup>30,31</sup> followed by subsequent reactions resulting in the  
322 formation of various products. Interestingly, this phenomenon has also been utilized for  
323 the investigation of electron-hopping in DNA by modifying guanine and adenine with  
324 cyclopropyl moieties.<sup>32,33</sup> Due to the instability of the initially formed closed ring radical  
325 cation, the modification results in rapid cyclopropyl ring-opening as well as 1,2-hydrogen  
326 migration, leading to the formation of an ionized allylamine.<sup>30,34</sup> Scission of the ring is  
327 followed either by a complete cleavage of the cyclopropyl moiety (TP246) or reaction of the  
328 ring opened radical cation with H<sub>2</sub>O/O<sub>2</sub>.<sup>32,34</sup> In the latter case, electron release from the

329 carbon centered radical followed by hydrolysis leads to the formation of a 3-  
330 hydroxypropanaminium cation<sup>35</sup> and subsequent addition of water results in the formation  
331 of the 3-hydroxypropanamide (TP318). In our system, TP288 is formed by photolytic  
332 cleavage of the hydroxymethyl group which leads to the formation of the acetamide  
333 product.<sup>35,36</sup> TP284 was most likely formed via H-atom abstraction, resulting in the  
334 formation of a neutral cyclopropyl radical followed by an electron transfer reaction and/or  
335 hydrolysis and elimination of water even though this reaction has only been shown to be  
336 catalyzed by enzymes so far.<sup>37,38</sup>

337  
338 Experiments with biomat material in the dark to determine the relative importance of  
339 biotransformation reactions indicated that microbial transformation of abacavir mainly  
340 occurred via oxidation of the primary alcohol group of the 2-cyclopenten-1-  
341 hydroxymethyl side chain to produce the corresponding carboxylic acid (abacavir  
342 carboxylate, Fig. S13). This was consistent with previous experiments conducted with  
343 mixed liquor suspended solids from an activated sludge treatment plant.<sup>39</sup>

344  
345 When abacavir was exposed simultaneously to light and microorganisms (Fig. 4), a rapid  
346 loss of abacavir was observed during the first 8-hour light period (i.e., the initial  
347 concentration decreased by approximately 90 %). For the next 16 hours (i.e., the dark  
348 period) abacavir removal was significantly slower. When the light was turned back on,  
349 nearly all remaining abacavir disappeared. As expected, the light-induced transformation of  
350 abacavir gave rise to the four photo-TPs described above (middle panel of Fig. 4). The  
351 concentrations of these photo-TPs decreased by approximately 25% over the next 2.5 days,  
352 indicating that further transformation took place, either via photolytic or microbial  
353 processes.

354 Additional biodegradation experiments with the four photo-TPs of abacavir revealed that  
355 biotransformation occurs at the same moiety as observed for the parent compound, leading  
356 to the corresponding carboxylates (TP246 carboxylate, TP284 carboxylate, TP288  
357 carboxylate and TP318 carboxylate; Fig. S20). Exact mass data and fragmentation patterns  
358 of bio-photo TPs determined by HRMS analysis are included in section 2.2 of the SI.  
359 Consequently, the observed decrease in concentration of photo-TPs shown in the middle



360 panel of Fig. 4 was mainly attributable to biotransformation, leading to a steady formation  
361 of carboxylate photo-TPs (bottom panel of Fig. 4). Faster transformation rates of abacavir  
362 photo-TPs observed during irradiation periods may have been attributable to enhanced  
363 biotransformation due to elevated oxygen concentrations or elevated pH values that  
364 occurred when the photosynthetic microorganisms in the biomat were active. Differences  
365 in biotransformation rates of TP246, TP284, TP288 and TP318, compared to abacavir (Fig.  
366 S14), indicate that alteration of chemical structure influences biotransformation kinetics,  
367 e.g. by affecting enzyme binding affinities or steric properties. Light-exposure of abacavir  
368 carboxylate formed in the dark led to its phototransformation, ultimately yielding the same  
369 photo-TPs as abacavir (bottom panel of Fig. 4). Considering that abacavir is already  
370 transformed extensively to abacavir carboxylate in activated sludge treatment,<sup>39</sup> a rapid  
371 elimination of both compounds can be expected in open-water unit process wetlands. In  
372 contrast to biotransformation reactions, similar phototransformation kinetics were  
373 observed for abacavir and abacavir carboxylate (Fig. S12). TP246 carboxylate was  
374 identified as the main product that accumulates over time because it is not susceptible to  
375 further reactions.

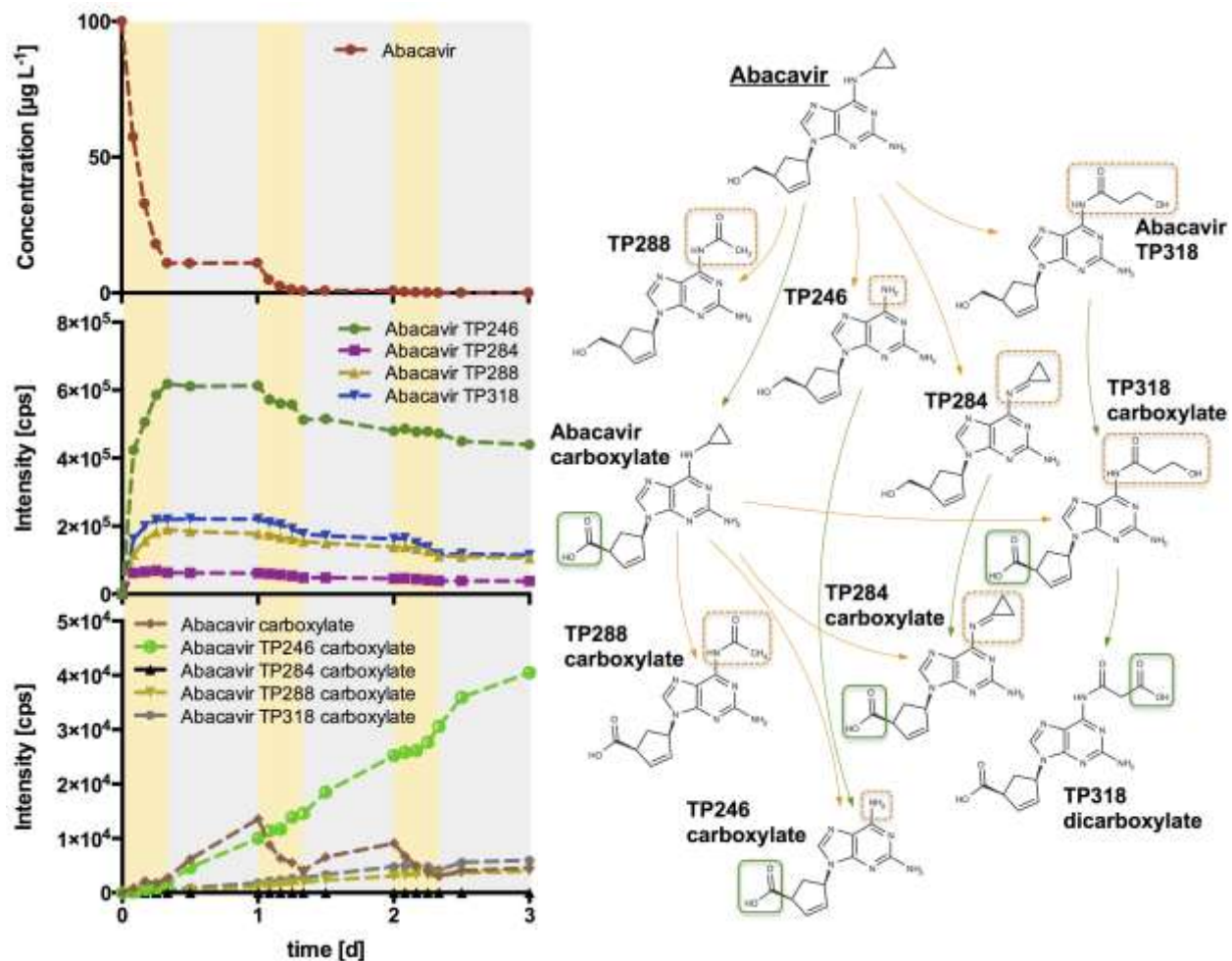


Figure 4. Transformation of abacavir (left, top) and resulting formation of photo-TPs (left, middle) and bio- / bio-photo-TPs (left, bottom) as well as proposed transformation pathway (right) in combined in 3 day experiments in the presence of biomat with 8 hours of daily irradiation. In the transformation pathway, photo- and biotransformation reactions and structural changes in the molecules are indicated in orange and green, respectively.

376

### 377 Transformation of acyclovir

378 In contrast to abacavir, the transformation of acyclovir was dominated by microbial  
 379 processes (Fig. 5), with biotransformation resulting in the formation of acyclovir  
 380 carboxylate, which was not susceptible to further microbial transformation. These results  
 381 are consistent with previous biotransformation experiments conducted with acyclovir in  
 382 sewage sludge.<sup>40</sup>

383 In the absence of biomat material, exposure of wetland water to simulated sunlight  
 384 resulted in formation of two main photo-TPs (TP257 and TP223). HRMS analysis indicated  
 385 that TP257 contains two additional oxygen atoms on the guanine moiety, as evidenced by

386 the detection of fragment m/z 184 instead of m/z 152 (Table S8; Fig. S16). Photosensitized  
387 degradation of guanine and guanosine occurs by reaction with excited triplet states,  $^1\text{O}_2$ ,  
388  $\cdot\text{OH}$  or  $\cdot\text{CO}_3^-$ .<sup>41,42</sup> The main product of the reaction of guanine with  $^1\text{O}_2$  has been identified  
389 as spiroiminodihydroantoin.<sup>43-45</sup> To assess the role of  $^1\text{O}_2$  in the phototransformation of  
390 acyclovir in wetland water, experiments were conducted in both  $\text{H}_2\text{O}$  and  $\text{D}_2\text{O}$  in the  
391 presence of the  $^1\text{O}_2$  sensitizer Rose Bengal (Fig. 5). Lifetimes of  $^1\text{O}_2$  in  $\text{D}_2\text{O}$  are more than an  
392 order of magnitude higher than in  $\text{H}_2\text{O}$  <sup>38</sup> and faster transformation of acyclovir in  $\text{D}_2\text{O}$   
393 confirmed the role of  $^1\text{O}_2$  for the indirect photolysis of acyclovir. In addition, the yield of  
394 TP257 increased in  $\text{D}_2\text{O}$ . Due to its photochemical properties acyclovir is likely to undergo  
395 self-sensitization via photoexcitation and subsequent formation of  $^1\text{O}_2$  as shown for guanine  
396 and guanosine.<sup>47-49</sup> For the second acyclovir photo-TP (TP223), HRMS analysis indicated  
397 the loss of two protons, most likely from the side chain, as evidenced by the detection of  
398 fragments m/z 152, 135 and 110, suggesting that the guanine moiety remained unchanged  
399 (Table S8). Additional information obtained from the fragmentation of the side chain was  
400 inconclusive but indicates oxidation of the terminal alcohol to the corresponding aldehyde  
401 via reaction with  $\cdot\text{OH}$ .<sup>50</sup>

402 Results from 72h simulated sunlight experiments conducted in the presence of the biomat  
403 revealed a steady decrease of acyclovir during light and dark periods, indicating the  
404 dominance of biotransformation processes (Fig. 5b). However, biotransformation of  
405 acyclovir was significantly faster in the sunlight experiments compared to dark controls  
406 (Fig. 5a&b) suggesting that the higher oxygen concentrations and the elevated pH values  
407 that occurred when microorganisms in the biomat were undergoing photosynthesis played  
408 a role in the biotransformation processes.<sup>10</sup> In the presence of simulated sunlight,  
409 production of the two phototransformation products (i.e., TP257 and TP224) was  
410 observed. No significant removal of TP257 was detected during dark periods, suggesting  
411 limited biotransformation via oxidation of the terminal hydroxyl-group of the side chain.  
412 Although the exact reason for this is unknown, a plausible explanation is that the structural  
413 modifications of the guanine core moiety prevented enzymatic oxidation of TP257. In  
414 contrast, concentrations of TP223 decreased in the dark. For the biotransformation  
415 product (i.e., acyclovir carboxylate), increasing concentrations were only observed during  
416 dark periods whereas its concentration decreased when exposed to sunlight. This indicates

417 that the compound was transformed further by photolytic processes, most likely via the  
 418 same mechanisms as acyclovir. This was confirmed by additional irradiation experiments  
 419 with acyclovir carboxylate in wetland water (results not shown).  
 420

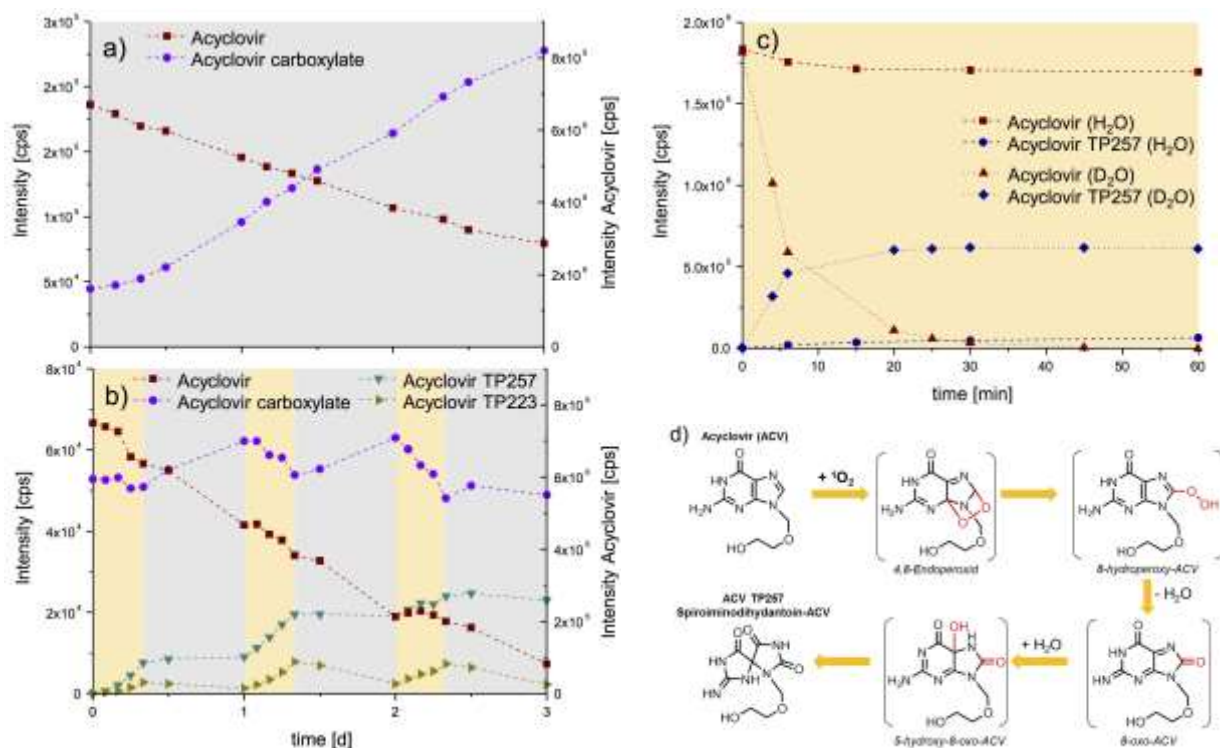


Figure 5. Transformation of acyclovir in the presence of biomat in the dark (a) in combined photo- and biotransformation experiments (b), as well as formation of TP257 via reaction of acyclovir with  $^1\text{O}_2$  in  $\text{D}_2\text{O}$  and  $\text{H}_2\text{O}$  using Rose Bengal as photosensitizer (c) and its proposed phototransformation pathway (d). The occurrence of acyclovir carboxylate at  $t_0$  in (a) and (b) is due to its emission by the WWTP that feeds the wetland.

421  
 422 Transformation of zidovudine, lamivudine and emtricitabine  
 423 MS spectra of the phototransformation products of emtricitabine, lamivudine and  
 424 zidovudine indicated structural changes at different positions on the molecules (Table S9-  
 425 S11). For lamivudine and emtricitabine, HRMS analysis revealed oxidation of the riboside  
 426 moiety (lamivudine TP245 and emtricitabine TP263), most likely via S-oxidation. This was  
 427 confirmed by comparison with commercially available reference standards. Addition of  
 428  $\text{H}_2\text{O}$  to the 5-fluoro-cytosine moiety was observed for emtricitabine (emtricitabine TP265).  
 429 Experiments conducted with the fluorine-free analogue lamivudine illustrates the  
 430 importance of fluorine substitution: the F-moiety increases the light absorbance at

431 wavelengths > 300 nm (Fig. S2) for emtricitabine and leads to faster photodegradation  
432 (Figure 1, Table S5). Emtricitabine TP265 was formed via hydration of the double bond of  
433 the 5-fluorocytosine moiety, yielding a hydroxyl-group at position C6. For zidovudine,  
434 observed phototransformations were mainly attributable to the photolability of the azido  
435 moiety. Formation of zidovudine TP239 can be explained by cleavage of N<sub>2</sub>, yielding a  
436 nitrene intermediate, which reacts further via intramolecular C-H insertion to an  
437 aziridine.<sup>51,52</sup> Subsequent nucleophilic attack of the aziridine by water leads to the  
438 hydroxylation of the C atom in β-position or the formation of a hydroxylamine (zidovudine  
439 TP257).<sup>51,53</sup> Results from HRMS analysis of zidovudine TP221 were inconclusive but  
440 indicated cleavage of N<sub>2</sub> and H<sub>2</sub>O from the furanosyl moiety.

441 In addition, photolytic cleavage of the nitrogen-carbon bond between the DNA base  
442 moieties and the riboside analogue side chains was observed for all three compounds,  
443 resulting in formation 5-fluoro-cytosine (emtricitabine TP129), cytosine (lamivudine  
444 TP111) and thymine (zidovudine TP126). None of these TPs were detected in sunlight  
445 experiments in the presence of biomat (Fig. S21-22), indicating that they were rapidly  
446 transformed, most likely via microbial processes. For zidovudine, this was confirmed by  
447 additional biodegradation experiments with the photo-TPs (i.e., thymine, TP239, TP257),  
448 showing the rapid elimination of thymine (Fig. S22). Considering the importance of both  
449 thymine and cytosine as DNA building blocks, it is likely that they were incorporated into  
450 the microbial biomass. The fate of 5-fluorocytosine remains unclear. Similar to abacavir  
451 and acyclovir, biotransformation of emtricitabine, lamivudine and zidovudine was shown  
452 to result in the formation of carboxylated TPs via oxidation of the terminal alcohol as  
453 already observed for abacavir and acyclovir (Fig. S13). As carboxylated TPs are expected to  
454 follow the same phototransformation mechanisms as the parent compounds,, the  
455 interactions of photo- and biotransformation reactions is likely to result in the complete  
456 elimination of via mineralization and/or microbial uptake (Fig. 6).

457  
458  
459  
460

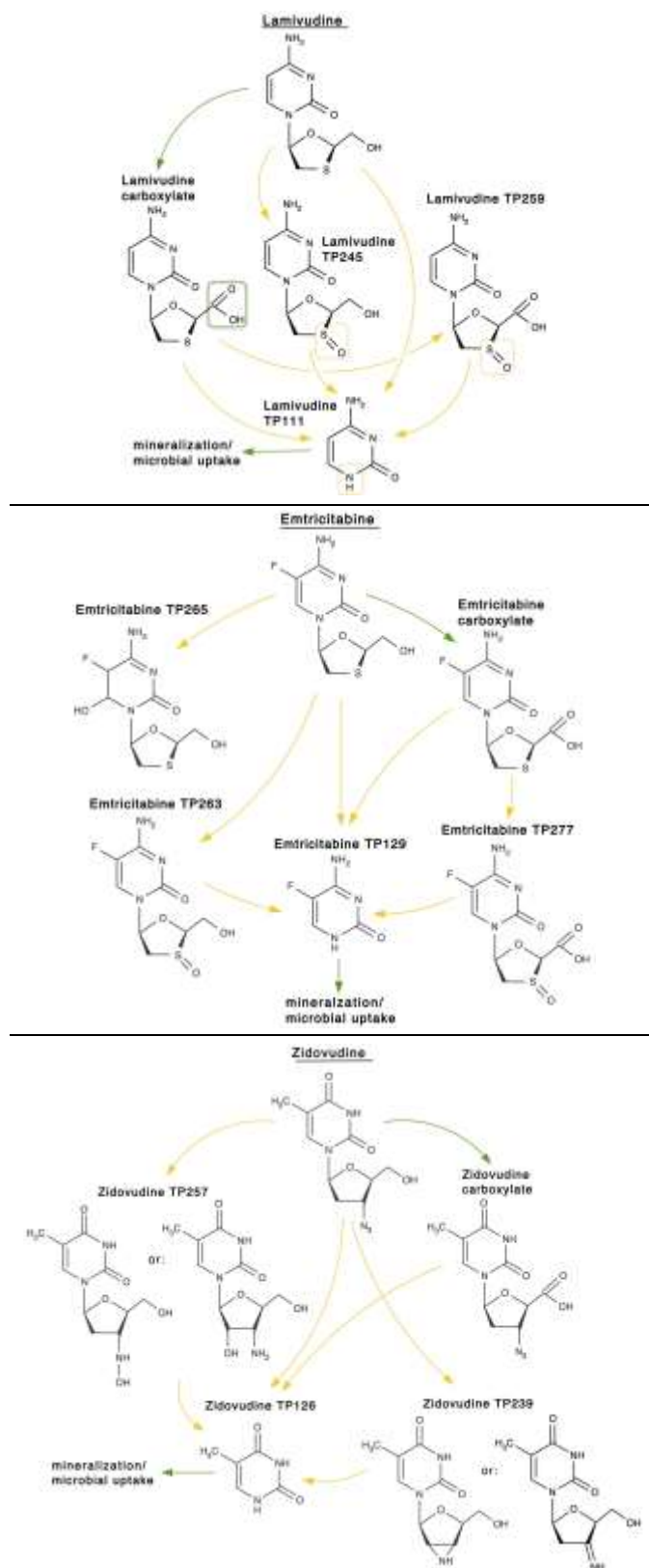


Figure 6. Proposed photo- and biodegradation pathway of lamivudine (top), emtricitabine (middle) and zidovudine (bottom) in open-water wetland cells. Orange and green

arrows indicate photo- and biotransformation reactions,  
respectively.

461

462 *Environmental implications*

463 The differences between kinetics and transformation product formation in presence and  
464 absence of the biomat highlight the complexity of transformation reactions that lead to the  
465 removal of trace organic contaminants in open water unit process wetlands and other  
466 sunlit waters. Attempts to predict the environmental fate of organic contaminants in these  
467 systems require an understanding of both processes as well as their potential interactions.

468 Identification of TPs showed that bio- and phototransformation reactions take place at  
469 different positions of the antiviral molecules. Phototransformation of biodegradation  
470 products was found to occur at the same location as in the parent compound. As a result,  
471 mechanisms and kinetics were similar to those observed for parent antiviral compounds.

472 This is important because carboxylate biodegradation products are typically present in  
473 much higher concentrations in biological treated wastewater compared to parent  
474 compounds.<sup>32</sup> In contrast, biodegradation kinetics of phototransformation products of  
475 antiviral drugs differed substantially from that observed for the parent compound even  
476 though the site of enzymatic oxidation did not change. This can be explained by differences  
477 in enzyme affinities and steric hindrance. For example, phototransformation of acyclovir  
478 created a transformation product (TP257) that was not susceptible to biotransformation  
479 by microorganisms that could oxidize the parent compound in the dark.

480 Combining kinetic studies with investigations of transformation product formation  
481 provides a better understanding of mechanisms relevant for the removal of trace organic  
482 contaminants in sunlit waters. By conducting biotransformation studies in the presence  
483 and absence of light it is possible to assess interactions between transformation processes  
484 and the likelihood that complete mineralization of trace organic contaminants will occur.  
485 These data also suggest that relative ratios of antiviral compounds and their  
486 transformation products might be useful as *in situ* probes to assess the relative importance  
487 of microbial and photochemical transformation pathways. This study also highlights the  
488 need to consider the formation of different transformation products in sunlit and light-  
489 shaded systems and the possibility of using knowledge of the reactivity of specific moieties

490 in chemical fate assessment. Considering the variety of formed transformation products,  
491 there is a need for appropriate risk assessment tools to assess potential adverse effects of  
492 transformation products with unknown toxicities on aquatic ecosystems. Finally, additional  
493 field studies are needed to further confirm the obtained laboratory results and to assess  
494 the suitability of the approach for the determination of the relative importance of  
495 individual transformation processes.

496

### 497 **Supporting Information**

498 Additional information on sample analysis; UV spectra of antiviral drugs; determination of  
499 indirect photolysis reaction rate constants, quantum yields, steady state concentrations of  
500 reactive intermediates in wetland water; experiments with DNA model compounds, MS<sup>n</sup>  
501 fragments of transformation products; formation and fate of abacavir photo-TPs by  
502 different reactive intermediates; results of combined bio- and phototransformation  
503 experiments with emtricitabine, lamivudine and zidovudine.

504

### 505 **Acknowledgement**

506 C.P. was supported by a postdoctoral scholarship of the German Academic Exchange  
507 Service (DAAD), J.W. by a scholarship of the Swiss National Science Foundation (PBEZP2-  
508 142887). Financial support by the Engineering Research Center for Reinventing the  
509 Nation's Water Infrastructure (ReNUWIt) EEC-1028968, and TransRisk, funded by the  
510 German Ministry of Science and Education, is gratefully acknowledged.

511

### 512 **References**

- 513 (1) Burrows, H.DI; Canle, M.; Santaballa, J.A.; Steenken, S. Reaction pathways and  
514 mechanisms of photodegradation of pesticides. *J. Photoch. Photobio. B* **2002**, 67(2),  
515 71-108.
- 516 (2) Boreen, A.L.; Arnold, W.A.; McNeill, K. Photodegradation of pharmaceuticals in the  
517 aquatic environment: A review. *Aquat. Sci.* **2003**, 65(4), 320-341.
- 518 (3) Halling-Sorensen, B.; Nielsen, S.N.; Lanzky, P.F.; Ingerslev, F.; Lutzhof, H.C.H.;  
519 Jorgensen, S.E. Occurrence, fate and effects of pharmaceutical substances in the  
520 environment - A review. *Chemosphere* **1998**, 36(2), 357-394.
- 521 (4) Onesios, K.M.; Yu, J.T.; Bouwer, E.J. Biodegradation and removal of pharmaceuticals  
522 and personal care products in treatment systems: a review. *Biodegradation* **2009**,  
523 20(4), 441-466.



- 524 (5) Lam, M.W.; Mabury, S.A. Photodegradation of the pharmaceuticals atorvastatin,  
525 carbamazepine, levofloxacin, and sulfamethoxazole in natural waters. *Aquat. Sci.*  
526 **2005**, 67(2), 177-188.
- 527 (6) Chiron, S.; Minero, C.; Vione, D. Photodegradation processes of the antiepileptic drug  
528 carbamazepine, relevant to estuarine waters. *Environ. Sci. Technol.* **2006**, 40(19),  
529 5977-5983.
- 530 (7) De Laurentiis, E.; Chiron, S.; Kouras-Hadef, S., Richard, C.; Minella, M.; Maurino, V.;  
531 Minero, C.; Vione, D. Photochemical fate of carbamazepine in surface freshwaters:  
532 Laboratory measures and modeling. *Environ. Sci. Technol.* **2012**, 46(15), 8164-8173.
- 533 (8) Kaiser, E.; Prasse, C.; Wagner, M.; Broeder, K.; Ternes, T.A. Transformation of  
534 oxcarbazepine and human metabolites of carbamazepine and oxcarbazepine in  
535 wastewater treatment and sand filters. *Environ. Sci. Technol.* **2014**, 48(17), 10208-  
536 10216.
- 537 (9) Jasper, J.T.; Nguyen, M.T. Jones, Z.L.; Ismail, N.S.; Sedlak, D.L., Sharp, J.O.; Luthy, R.G.,  
538 Horne, A.J.; Nelson, K.L. Unit process wetlands for removal of trace organic  
539 contaminants and pathogens from municipal wastewater effluents. *Environ. Engin.*  
540 *Sci.* **2013**, 30(8), 421-436.
- 541 (10) Jasper, J.T.; Sedlak, D.L. Phototransformation of wastewater-derived trace organic  
542 contaminants in open-water unit process treatment wetlands. *Environ. Sci. Technol.*  
543 **2013**, 47(19), 10781-10790.
- 544 (11) Nguyen, M.T.; Silverman, A.I.; Nelson, K.L. Sunlight inactivation of MS2 coliphage in  
545 the absence of photosensitizers: Modeling the endogenous inactivation rate using a  
546 photoaction spectrum. *Environ. Sci. Technol.* **2014**, 48(7), 3891-3898.
- 547 (12) Silverman, A.I.; Nguyen, M.T.; Schilling, I.E.; Wenk, J.; Nelson, K.L. Sunlight  
548 inactivation of viruses in open-water unit process treatment wetlands: Modeling  
549 endogenous and exogenous inactivation rates. *Environ. Sci. Technol.* **2015**, 49(5),  
550 2757-2766.
- 551 (13) Jasper, J.T.; Jones, Z.L.; Sharp, J.O.; Sedlak, D.L. Biotransformation of trace organic  
552 contaminants in open-water unit process treatment wetlands. *Environ. Sci. Technol.*  
553 **2014**, 48(9), 5136-5144.
- 554 (14) Jasper, J.T.; Jones, Z.L.; Sharp, J.O.; Sedlak, D.L. Nitrate removal in shallow, open-  
555 water treatment wetlands. *Environ. Sci. Technol.* **2014**, 48(19), 11512-11520.
- 556 (15) Wood, T.P.; Duvenage, C.S.J.; Rohwer, E. The occurrence of anti-retroviral  
557 compounds used for HIV treatment in South African surface water. *Environ. Pollut.*  
558 **2015**, 199, 235-243.
- 559 (16) Peng, X.; Wang, C.; Zhang, K.; Wang, Z.F.; Huang, Q.X.; Yu, Y.Y.; Ou, W.H. Profile and  
560 behavior of antiviral drugs in aquatic environments of the Pearl River Delta, China.  
561 *Sci. Total Environ.* **2014**, 466, 755-761.
- 562 (17) Prasse, C.; Schluesener, M.P.; Schulz, R.; Ternes, T.A. Antiviral drugs in wastewater  
563 and surface waters: A new pharmaceutical class of environmental relevance?  
564 *Environ. Sci. Technol.* **2010**, 44(5), 1728-1735.
- 565 (18) Azuma, T.; Nakada, N.; Yamashita, N.; Tanaka, H. Synchronous dynamics of observed  
566 and predicted values of anti-influenza drugs in environmental waters during a  
567 seasonal influenza outbreak. *Environ. Sci. Technol.* **2012**, 46(23), 12873-12881.
- 568 (19) Wommack, K.E.; Colwell, R.R. Virioplankton: Viruses in aquatic ecosystems.  
569 *Microbiol. Mol. Biol. R.* **2000**, 64(1), 69-114.

- 570 (20) Dulin, D.; Mill, T. Development and evaluation of sunlight actinometers. *Environ. Sci.*  
571 *Technol.* **1982**, 16(11), 815-820.
- 572 (21) Grebel, J. E.; Pignatello, J. J.; Mitch, W. A. Sorbic acid as a quantitative probe for the  
573 formation, scavenging and steady-state concentrations of the triplet-excited state of  
574 organic compounds. *Water Res.* **2011**, 45(19), 6535–6544.
- 575 (22) Boreen, A.L.; Edhlund, B.L.; Cotner, J.B.; McNeill, K. Indirectphotodegradation of  
576 dissolved free amino acids: The contribution of singlet oxygen and the differential  
577 reactivity of DOM from various sources. *Environ. Sci. Technol.* **2008**, 42(15),  
578 5492–5498.
- 579 (23) Packer, J. L.; Werner, J.J.; Latch, D.E.; McNeill, K.; Arnold, W.A. Photochemical fate of  
580 pharmaceuticals in the environment: Naproxen, diclofenac, clofibrac acid, and  
581 ibuprofen. *Aquat. Sci.* **2003**, 65(4), 342–351.
- 582 (24) Vione, D.; Khanra, S.; Man, S.C.; Maddigapu, P.R.; Das, R.; Arsene, C.; Olariu, R.-I.;  
583 Maurino, V.; Minero, C. Inhibition vs. enhancement of the nitrate-induced  
584 phototransformation of organic substrates by the (OH)-O-center dot scavengers  
585 bicarbonate and carbonate. *Water Res.* **2009**, 43(18), 4718-4728.
- 586 (25) Canonica, S.; Kohn, T.; Mac, M.; Real, F.J.; Wirz, J.; Von Gunten, U. Photosensitizer  
587 method to determine rate constants for the reaction of carbonate radical with  
588 organic compounds. *Environ. Sci. Technol.* **2005**, 39(23), 9182-9188.
- 589 (26) Bedini, A.; De Laurentiis, E.; Sur, B.; Maurino, V.; Minero, C.; Brigante, M.; Mailhot, G.;  
590 Vione, D. Phototransformation of anthraquinone-2-sulphonate in aqueous solution.  
591 *Photochem. Photobio. S.* **2012**, 11(9), 1445-1453.
- 592 (27) Zepp, R.G.; Hoigne, J.; Bader, H. Nitrate-induced photooxidation of trace organic  
593 chemicals in water. *Environ. Sci. Technol.* **1987**, 21, 443-450.
- 594 (28) Burns, J.M.; Cooper, W.J.; Ferry, J.L.; King, D.W.; DiMento, B.P.; McNeill, K.; Miller, C.J.;  
595 Miller, W.L.; Peake, B.M.; Rusak, S.A.; Rose, A.L.; Waite, T.D. Methods for reactive  
596 oxygen species (ROS) detection in aqueous environments. *Aquat. Sci.* **2012**, 74(4),  
597 683-734.
- 598 (29) Sakkas, V.A.; Lambropoulou, D.A.; Albanis, T.A. Photochemical degradation study of  
599 irgarol 1051 in natural waters: influence of humic and fulvic substances on the  
600 reaction. *J. Photoch. Photobio. A* **2002**, 147(2), 135-141.
- 601 (30) Bouchoux, G.; Alcaraz, C.; Dutuit, O.; Nguyen, M.T. Unimolecular chemistry of the  
602 gaseous cyclopropylamine radical cation. *J. Am. Chem. Soc.* **1998**, 120(1), 152-160.
- 603 (31) Cooksy, A.L.; King, H.F.; Richardson, W.H. Molecular orbital calculations of ring  
604 opening of the isoelectronic cyclopropylcarbiny radical, cyclopropoxy radical, and  
605 cyclopropylaminium radical cation series of radical clocks. *J. Org. Chem.* **2003**,  
606 68(24), 9441-9452.
- 607 (32) Nakatani, K.; Dohno, C.; Saito, I. Design of a hole-trapping nucleobase: Termination  
608 of DNA-mediated hole transport at N-2-cyclopropyldeoxyguanosine. *J. Am. Chem.*  
609 *Soc.* **2001**, 123(39), 9681-9682.
- 610 (33) Shao, F.W.; O'Neill, M.A.; Barton, J.K. Long-range oxidative damage to cytosines in  
611 duplex DNA. *P. Natl. Acad. Sci. USA* **2004**, 101(52), 17914-17919.
- 612 (34) Qin, X.Z.; Williams, F. Electron-spin-resonance studies on the radical cation  
613 mechanism of the ring-opening of cyclopropylamines. *J. Am. Chem. Soc.* **1987**,  
614 109(2), 595-597.

- 615 (35) Paul, M.M.S.; Aravind, U.K.; Pramod, G.; Saha, A.; Aravindakumar, C.T. Hydroxyl  
616 radical induced oxidation of theophylline in water: a kinetic and mechanistic study.  
617 *Org. Biomol. Chem.* **2014**, 12(30), 5611-5620.
- 618 (36) Goutailler, G.; Valette, J.C.; Guillard, C.; Paisse, O.; Faure, R. Photocatalysed  
619 degradation of cyromazine in aqueous titanium dioxide suspensions: comparison  
620 with photolysis. *J. Photoch. Photobio. A* **2001**, 141(1), 79-84.
- 621 (37) Shaffer, C.L.; Morton, M.D.; Hanzlik, R.P. N-dealkylation of an N-cyclopropylamine by  
622 horseradish peroxidase. Fate of the cyclopropyl group. *J. Am. Chem. Soc.* **2001**,  
623 123(35), 8502-8508.
- 624 (38) Cerny, M.A.; Hanzlik, R.P. Cytochrome P450-catalyzed oxidation of N-benzyl-N-  
625 cyclopropylamine generates both cyclopropanone hydrate and 3-  
626 hydroxypropionaldehyde via hydrogen abstraction, not single electron transfer. *J.*  
627 *Am. Chem. Soc.* **2006**, 128(10), 3346-3354.
- 628 (39) Funke, J.; Prasse, C.; Ternes T.A. Identification and fate of transformation products of  
629 antiviral drugs formed during biological wastewater treatment (submitted).
- 630 (40) Prasse, C.; Wagner, M.; Schulz, R.; Ternes, T.A. Biotransformation of the antiviral  
631 drugs acyclovir and penciclovir in activated sludge treatment. *Environ. Sci. Technol.*  
632 **2011**, 45(7), 2761-2769.
- 633 (41) Cadet, J.; Douki, T.; Gasparutto, D.; Ravanat, J.L. Oxidative damage to DNA: formation,  
634 measurement and biochemical features. *Mutat. Res. - Fund. Mol. M.* **2003**, 531(1-2),  
635 5-23.
- 636 (42) Neeley, W.L.; Essigmann, J.M. Mechanisms of formation, genotoxicity, and mutation  
637 of guanine oxidation products. *Chem. Res. Toxicol.* **2006**, 19(4), 491-505.
- 638 (43) Cui, L.; Ye, W.; Prestwich, E.G.; Wishnok, J.S.; Taghizadeh, K.; Dedon, P.C.;  
639 Tannenbaum S.R. Comparative analysis of four oxidized guanine lesions from  
640 reactions of DNA with peroxyxynitrite, singlet oxygen and  $\gamma$ -radiation. *Chem. Res.*  
641 *Toxicol.* **2012**, 26(2), 195-202
- 642 (44) Luo, W.; Muller, J.G.; Rachlin, E.M.; Burrows, C.J. Characterization of  
643 spiroiminodihydantoin as a product of one-electron oxidation of 8-oxo-7,8-  
644 dihydroguanosine. *Org. Lett.* **2000**, 2(5), 613-616.
- 645 (45) Cadet, J.; Douki, T.; Ravanat, J.L. Oxidatively generated damage to the guanine moiety  
646 of DNA: Mechanistic aspects and formation in cells. *Accounts Chem. Res.* **2008**, 41(8),  
647 1075-1083.
- 648 (46) Rodgers, M. A. J.; Snowden, P. T. Lifetime of  $O_2(1\Delta_g)$  in liquid water as determined by  
649 time-resolved infrared luminescence measurements. *J. Am. Chem. Soc.* **1982**,  
650 104(20), 5541-5543.
- 651 (47) Mohammad, T.; Morrison, H. Evidence for the photosensitized formation of singlet  
652 oxygen by UVB irradiation of 2'-deoxyguanosine 5'-monophosphate. *J. Am. Chem.*  
653 *Soc.* **1996**, 118(5), 1221-1222.
- 654 (48) Redmond, R.W.; Gamlin, J.N. A compilation of singlet oxygen yields from biologically  
655 relevant molecules. *Photochem. Photobiol.* **1999**, 70(4), 391-475.
- 656 (49) Torun, L.; Morrison, H. Photooxidation of 2'-deoxyguanosine 5'-monophosphate in  
657 aqueous solution. *Photochem. Photobiol.* **2003**, 77(4), 370-375.
- 658 (50) von Gunten, U. Ozonation of drinking water: Part I. Oxidation kinetics and product  
659 formation. *Water Res.* **2003**, 37(7), 1443-1467.

- 660 (51) Dunge, A.; Chakraborti, A.K.; Singh, S. Mechanistic explanation to the variable  
661 degradation behaviour of stavudine and zidovudine under hydrolytic, oxidative and  
662 photolytic conditions. *J. Pharmaceut. Biomed.* **2004**, 35(4), 965-970.
- 663 (52) Gritsan, N.; Platz M. Photochemistry of azides: The azide/nitrene interface. In  
664 *Organic Azides: Syntheses and Applications*; Bräse, S., Banert, K., Eds.; John Wiley &  
665 Sons; 2010, pp 311-372.
- 666 (53) Iwamoto, T.; Hiraku, Y.; Oikawa, S.; Mizutani, H.; Kojima, M.; Kawanishi, S. Oxidative  
667 DNA damage induced by photodegradation products of 3'-azido-3'-deoxythymidine.  
668 *Archives of Biochemistry and Biophysics.* 2003;416(2):155-163.  
669